FAST LOW-COST SINGLE ELEMENT ULTRASOUND REFLECTIVITY TOMOGRAPHY USING ANGULAR DISTRIBUTION ANALYSIS.

Andrey Kuzmin[⋆] *Xiang Zhang*[†] *Jonathan Fincke*[†] *Micha Feigin*[†]
Brian W. Anthony[†] Victor Lempitsky[⋆]

[⋆]Skolkovo Institute of Science and Technology, Russia
[†]Department of Mechanical Engineering, Massachusetts Institute of Technology, USA

ABSTRACT

We propose a new reconstruction method for ultrasound reflectivity tomography. Our imaging setup is based around a single imaging and sensing element travelling along the perimeter of a circular the domain. A 2D reflectivity field of the interior of the domain is recovered based on back-scattered echoes recorded at a large number of element positions. To obtain high-quality images, we suggest a simple new approach to resolve the angular ambiguity inherent to the ultrasound measurements based on circular wave-fronts. The analysis incorporates observations obtained at several adjacent positions of a sensing elements. The method is validated using simulated and real data of a human limb. The validation shows improvement of the image quality compared to the classical image reconstruction algorithm for such setups.

Index Terms— ultrasound reflection tomography, tomographic image reconstruction, limb ultrasound imaging

1. INTRODUCTION

Ultrasound tomography (UST) is a recent imaging modality for imaging of soft tissues. Recent systems based on the combination of transmission and reflection tomography based on a large number of sensors and emitters have produced clinically relevant images of soft tissues with quality and resolution comparable to those of MRI [1, 2]. In this work we aim to develop an imaging algorithm for a much simpler and low-cost imaging setup containing a single moving imaging element.

The use of single transceiving element restricts the class of methods that can be employed to reflection-based tomography, and we resort to the use of wide fan-out transcieving element to increase the coverage capability of the system. Application-wise, we further increase the difficulty of the imaging problem by considering the limb imaging task that implies imaging not only soft tissues but also bone surfaces. Generally, scans of soft tissue with bone presents an interesting set of new imaging challenges and applications [3].

The traditional reconstruction algorithms based on weak scattering model [4, 5] suffer from artifacts that are caused by the circular integration paths implied by the omnidirectional sound wavefront propagation. The artifacts include the overall bluriness of the recovered images as well as halo-type effects around strongly reflecting surfaces. Our approach aims to reduce the amount and intensity of the artifacts by restricting circular integration paths. The additional information on the reflected pulse direction is obtained from the local analysis that is aimed to resolve the angular ambiguty that is associated with the propagating wave-fronts.

Our analysis uses a series of local convolutions with directional filters. The result of such filtering provides an *angular distribution* that assigns higher values to the directions that are likely to correspond to scatterers that generate a certain signal recorded for a certain traveltime by a transciever at a certain location. A post-processing procedure based on the *softmax* function is applied to each angular distribution in order to emphasize directions of high probability. The reconstruction is performed by aggregating back-projected reflectance values into the circular coordinate system according to the estimated angular probabilities. We demonstrate considerable image quality improvement from the use of our analysis both on real and synthetic data.

2. METHODS

Experimental setup. A single element ultrasound system with a circular geometry (figure 1 (a)) has been designed and built to support iterative development of algorithms for the above target applications [6]. A single element emitting and scanning with one receive channel has been chosen in the pursuit of a simple and low-cost solution.

During the scan the transcieving element follows a circular path. At each location along the path, a sampled version of the reflection amplitude in time (figure 1 (b)) called the *A-line* is recorded. Each value in the A-line thus corresponds to a certain traveltime. A-lines for multiple locations are then stacked into a two dimensional image (figure 1 (c)).

A calibration procedure [6] is used to map the traveltime values into distances (using an average estimate of the sound speed). After such mapping, the input to the reconstruction
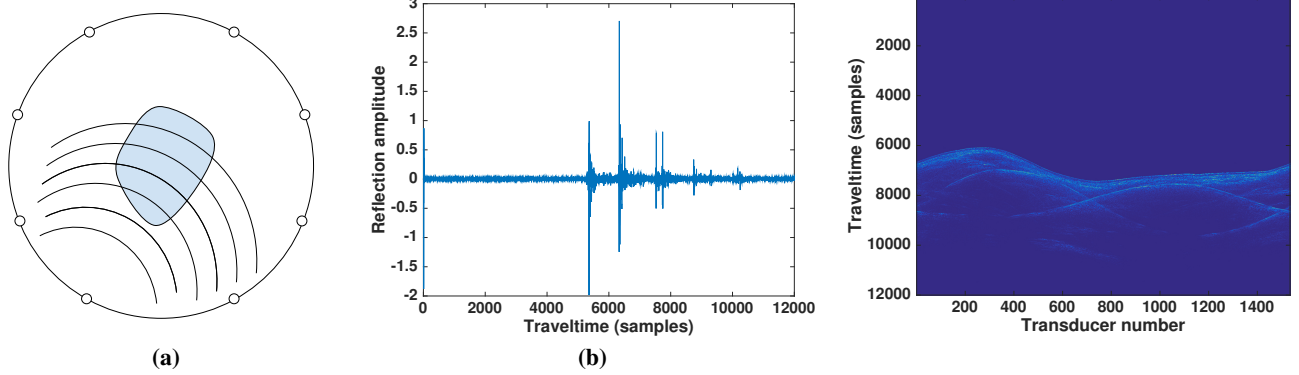
Fig. 1. Tomography system geometry and data. (a) Circular ring geometry of the tomography system. Transciever locations are equally spaced along the circular path. (b) Example of a real A-line signal. Reflected pulse is recorded at the point coincident with the source position. (c) Example of real data: array of A-line is stacked into a single 2D image.

algorithm is an image $I(r, j)$, where r corresponds to the distance between the element and the reflectors inside the tank, and j denotes the position of the scanning element along the circular path.

Alongside the (r, j) coordinate system (the *data space*), we consider the coordinates (x, y) in the device coordinate system (*the object space*). There is no direct mappings between the two coordinate systems. A single (r, j)-pair corresponds to a circular arc $A(r, j)$ in the (x, y) (object) space, containing points at the same distance r from the reflector position (fig. 3a). The fan-out (angular length) of the arc is determined by the characteristics of the imaging element and is considered known. Likewise, a single reflector located at point (x, y) in the object space traces a sinusoid in the (r, j) object space. The task of the tomographic reconstruction is then to reproject the intensity observed in the data space into the object space.

Angular distribution analysis. The family of methods based on the circular paths integrals [4, 5] back-project the intensity at (r, j) into the data space by spreading it uniformly across the entire arc $A(r, j)$. They thus make an unrealistic assumption that a signal picked up at (r, j) is caused in equal measure by a set of reflectors located along the entire arc. In contrast to this approach, we present a method that estimates a non-uniform angular distribution and demonstrate how it leads to an improved image quality.

To estimate the angular distribution, for each arc we consider each point $p(\Theta; r, j) \in A(r, j)$ parameterized by the angle Θ with the radius-vector from the element position to the center of the circle. Each of $p(\Theta; r, j)$ backprojects into a sinusoid line $S(\Theta; r, j)$ in the data space, and the resulting family of sinusoids naturally intersects at (r, j) (fig. 3b).

Our analysis is based on a highly-plausible assumption that a strong reflector located at the point $p(\Theta; r, j) \in A(r, j)$ is likely to cause a strong signal response for a certain range of adjacent locations of the transducer $j' \in [j - \delta, j + \delta]$. When the assumption holds, a large value of the integral along

the local part of the sinusoid $S(\Theta; r, j)$ around (r, j) is to be observed. For (r, j) that correspond to a high value in $I(r, j)$ this assumption can be used to identify which of the $p(\Theta; r, j)$ are more likely to contain reflectors.

Reconstruction algorithm. We construct a family of directional filters by bounding the family of sinusoids to the window around (r, j) (fig. 3 (b)). The obtained filter bank is then convolved with the corresponding image patch in order to estimate the angular distribution for the current point (see fig. 3 (c)):

$$\tilde{p}(\Theta; r, j) = T(r, j) * f_{t,\Theta}, \tag{1}$$

Here $T(r, j)$ denotes the patch of the input image centered at (r, j), and $f_{t,\Theta}$ is a filter approximating the sinusoid (or more precisely the indicator function of the intersection of the sinusoid $S(\Theta; r, j)$ and the local window).

The obtained (unnormalized) distribution $\tilde{p}(\Theta; r, j)$ is then passed through a softmax normalization:

$$p(\Theta; r, j) = \frac{\exp\left(\alpha \tilde{p}(\Theta; r, j)\right)}{\int_{\Phi} \exp\left(\alpha \tilde{p}(\Phi; r, j)\right) d\Phi} \tag{2}$$

and the resulting distribution $p(\Theta; r, j)$ is then used to perform a back-projection from data space to image space:

$$R(x, y) = \sum_{(x,y)=p(\Theta; r, j)} I(r, j) p(r, j, \Theta), \tag{3}$$

i.e. the intensity at (x, y) is accumulated from (r, j) such that $(x, y) \in A(r, j)$, and the contribution from such (r, j) is proportional to the intensity $I(r, j)$ weighted by the corresponding angular distribution.

The constant α in (2) controls the tradeoff between the sharpness of the resulting reconstruction and its robustness to noise. In the limit $\alpha \to +\infty$, the resulting normalized distribution represents a delta function, which assigns the full intensity $I(r, j)$ to a single point $p(\Theta; r, j)$ with $\Theta = \arg\max_{\Theta} \tilde{p}(\Theta; r, j)$. We refer to this method as *the*
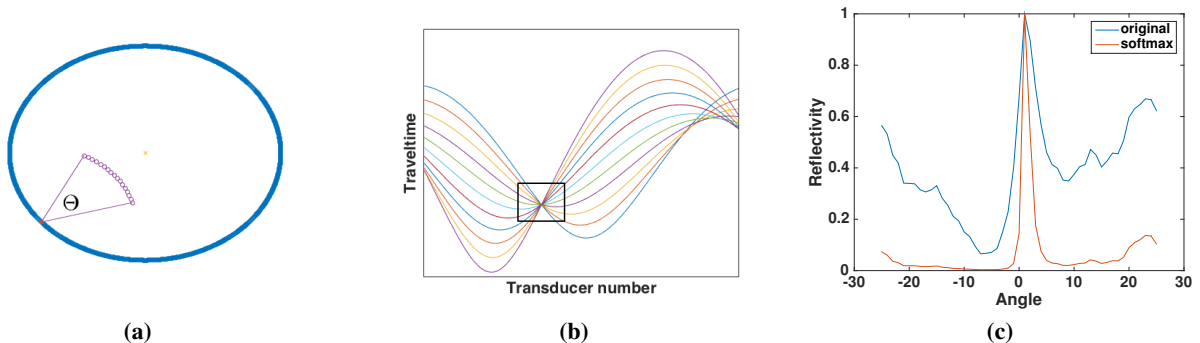
Fig. 2. Schematic view of our reconstruction algorithm. (a) The circular arc corresponding to different angles. (b) The set of PSF functions corresponding to each point of the circular arc (c) Example of an angular distribution and its post-processed version after applying $softmax$ function.

dominant orientation reconstruction through the rest of the paper. At the other extreme, for $\alpha = 0$ we recover the classical algorithm based on the uniform angular distribution.

We note that both the angular distribution analysis step (1) and the image reconstruction step (3) are data parallel in nature allowing to efficiently employ modern parallel architectures.

3. EXPERIMENTAL VALIDATION

Below we evaluate our method for a synthetic experiment with known ground truth data. Two reconstructions based on real patient data are also presented. Generally, we compare three methods corresponding to the classical backprojection based on uniform angular distribution, the dominant orientation recosntruction and the full distribution estimated with our analysis respectively.

Synthetic phantom experiment. This section contains results based on the time-domain simulation of the sound wave reflection. Simulations are performed using K-wave toolbox [7]. We construct a two-dimensional medium of elliptic geometry that aims to reproduce strong reflection from a bone. Sound speed 1800 m/s is used for the interior of the ellipse and 1509 m/s for the surrounding domain respectively. The enveloped single frequency tone burst at 5 MHz is used to gather the reflection data at each of 1500 transducer locations, each A-line consists of 1000 samples recorded. The reflecting boundary shape and the corresponding reconstruction results are presented in 3 (b-d). We add Gaussian noise to the input data in order to assess robustness of our method to the noise level. The results in 3 (f-h) demonstrate better reconstruction for both methods based on full angular distribution.

Real data experiments. This section is based on the real data obtained from the circular ring tomography system described in [6]. The corresponding reflection data has the dimensions of 1500 transducer locations and 10000 time samples in each A-line.

We present results of reconstruction for two scans of real scans for two healthy volunteers in fig. 4. Each scan is a two-dimensional perpendicular slice of an arm approximately 15 cm below the elbow. The reconstructions performed with the classical method shown in fig.4 (a,d) show many artifacts around plausible positions of the strong reflectors. Our method based on the dominant orientation (fig.4 (b,e)) doesn't suffer from the presence of the artifacts however it leads to higher noise level on the resulting images. The balance is achieved with the full angular distribution method (fig.4 (c,f)) demonstrates significant quality improvement over the first two methods and leads to display of additional details in the reconstructed reflectivity fields.

Computational performance. Our unoptimized MATLAB implementation of the reconstruction algorithm computes a single reconstruction within approximately 20 min for the full angular distribution. This timing suggests that efficient GPU parallelization may perform the reconstruction in a time comparable with the duration of data acquisition (which is approximately two seconds in our setup).

4. SUMMARY

A new reconstruction method for ultrasound reflectivity tomography is proposed. We perform back-projection to the device geometry based on angular distribution analysis. The angular distribution provides weights that allow to map each sample of the reflection data to the points of device geometry in a more accurate way. Two specific methods based on different usage of the angular distribution are considered. All the considered methods are fast and allow efficient parallelization.

The proposed method outperforms the standard circular path-integration back-projection method showing less artifacts and higher level of detail. This is evidenced by an experiment with synthetic data as well as for two reconstructions with real data corresponding to human arms.
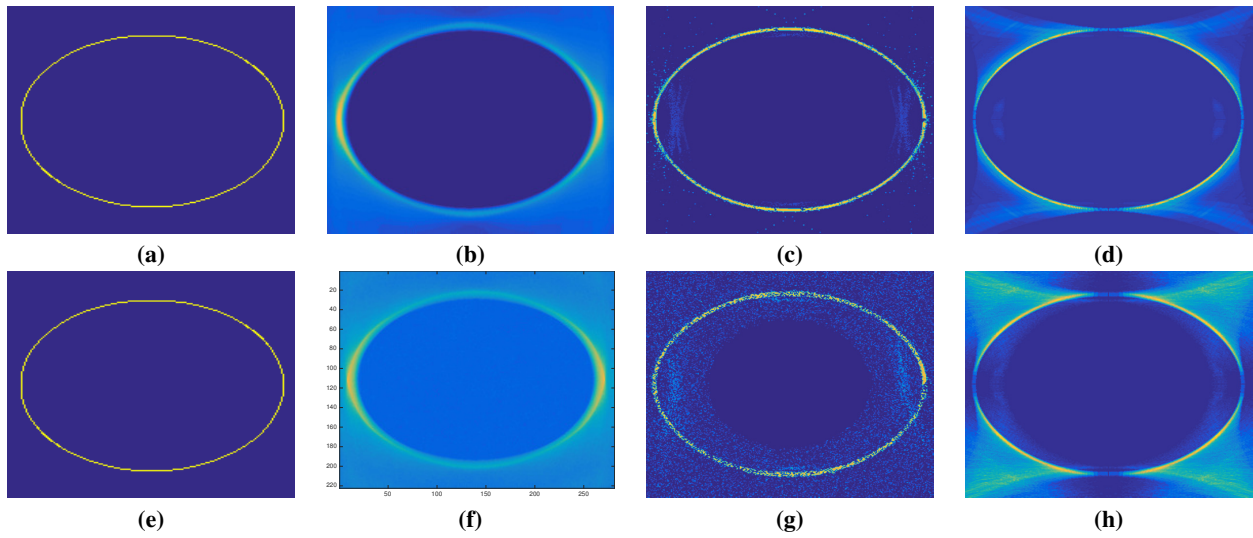
Fig. 3. Reconstruction results based on simulation for a medium with a strong sound speed variation. (a,e) Ground truth boundary shape. Reconstruction of the reflectivity using (b,f) uniform distribution (c,g) dominant orientation (d,h) full distribution. The second row shows reconstruction results for the synthetic reflection data with an additional level of noise

.
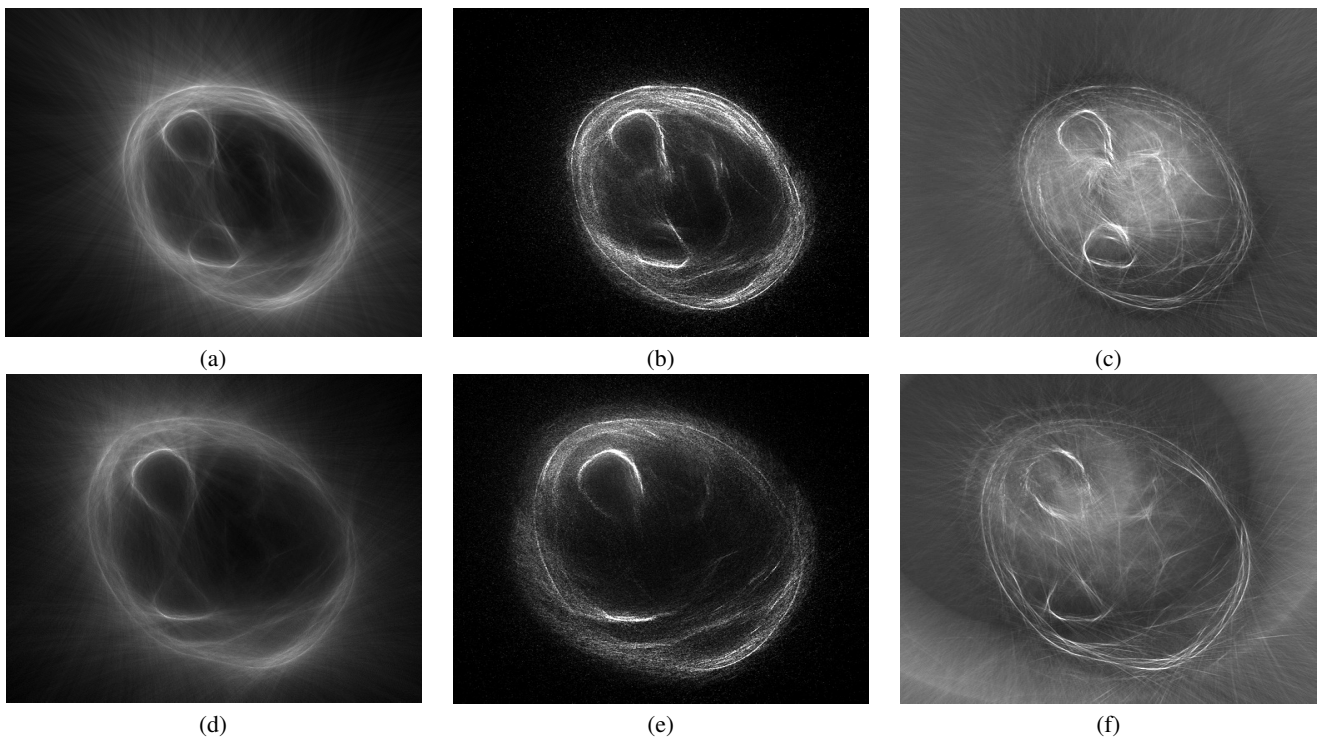
Fig. 4. Arm reflectivity reconstruction results for two healthy volunteers (the first row (a-c) and the second row (d-f) correspond to the first and the second scan respectively)). First column (a,d), second column (b,e) and the third column (c,f) correspond to reconstruction based on the uniform distribution, dominant orientation and the full distribution respectively.

5. REFERENCES

[1] Nebojsa Duric, Peter Littrup, Lou Poulo, Alex Babkin, Roman Pevzner, Earle Holsapple, Olsi Rama, and Carri Glide, "Detection of breast cancer with ultrasound tomography: First results with the computed ultrasound risk evaluation (cure) prototype," *Medical physics*, vol. 34, no. 2, pp. 773–785, 2007.

[2] Torsten Hopp, Lukas Šroba, Michael Zapf, Robin Dapp, Ernst Kretzek, Hartmut Gemmeke, and Nicole V Ruiter, "Breast imaging with 3d ultrasound computer tomography: Results of a first in-vivo study in comparison to mri images," in *Breast Imaging*, pp. 72–79. Springer, 2014.

[3] Pascal Laugier and Guillaume Haat, *Bone Quantitative Ultrasound*, Springer Science & Business Media, Nov. 2010.

[4] Stephen J Norton and Melvin Linzer, "Ultrasonic reflectivity tomography: reconstruction with circular transducer arrays," *Ultrasonic Imaging*, vol. 1, no. 2, pp. 154–184, 1979.

[5] Stephen J Norton, "Reconstruction of a two-dimensional reflecting medium over a circular domain: Exact solution," *The Journal of the Acoustical Society of America*, vol. 67, no. 4, pp. 1266–1273, 1980.

[6] Xiang Zhang, Jonathan Fincke, Andrey Kuzmin, Victor Lempitsky, and Brian W. Anthony, "A single element 3d ultrasound tomography system," in *Proc. of 37th annual conference of the IEEE Engineering in Medicine and Biology Society*.

[7] Bradley E Treeby and Benjamin T Cox, "k-wave: Matlab toolbox for the simulation and reconstruction of photoacoustic wave fields," *Journal of biomedical optics*, vol. 15, no. 2, pp. 021314–021314, 2010.